ELSEVIER

International Journal of Solids and Structures 41 (2004) 4457–4472

INTERNATIONAL JOURNAL OF SOLIDS and STRUCTURES

www.elsevier.com/locate/ijsolstr

Dynamic analysis of composite plates subjected to multi-moving loads based on a third order theory

Sang-Youl Lee [a,*], Sung-Soon Yhim [b]

[a] Department of Civil and Environmental Engineering, Massachusetts Institute of Technology, Cambridge, MA 02139, USA
[b] Department of Civil Engineering, University of Seoul, 90 Junneoung-Dong, Dongdaemoon-Gu, Seoul 130-743, South Korea

Received 21 October 2003; received in revised form 22 March 2004
Available online 23 April 2004

Abstract

This study reports on a dynamic analysis of single and two-span continuous composite plate structures subjected to multi-moving loads. Third order transverse shear deformation and rotary inertia in laminated composite plates under the moving loads are studied. The 7-DOF finite element model of composite plate described in this paper may allow us not only to determine the dynamic response under the moving loads but also to analyze the influences on dynamic behavior of different plate theories, layup sequences, and boundaries. The numerical results demonstrate significant effects of the ply angles on the dynamic behaviors of composite structures under the moving loads as well as the criticality of the third order shear deformation theory (TSDT) from the standpoints of computational accuracy. Furthermore, the results reported in this paper show the interactions between ply angels and moving velocities. Key observation points are discussed and a brief design guideline is given.

Keywords: Composite materials; Moving loads; Finite element analysis; Third order plate theory

1. Introduction

Theoretical and experimental studies of the dynamic behavior of various civil structures such as bridges and roads subject to moving vehicles have been conducted for more than one and half centuries. Theoretically, the problem of a moving load was first tackled for the case, in which the beam mass was considered small against the mass of a single, constant load. The original approximation solution was proposed by Willis (1849) and Stokes (1849), one of the early experimenters in the field. In the twentieth century, beam problems caused by the moving loads in idealized vibrations up on the railway bridges were studied by Timoshenko (1922), Jeffcott (1929), Lowan (1935), and Looney (1958). Biggs (1959) conducted several field investigations and theoretical studies related to the dynamic behaviors of bridges with idealized one

* Corresponding author. Tel.: +1-617-258-8366.
E-mail addresses: leesy@mit.edu, leesangyoul@hanmail.net (S.-Y. Lee).

0020-7683/$ - see front matter © 2004 Elsevier Ltd. All rights reserved.
doi:10.1016/j.ijsolstr.2004.03.021

Nomenclature

u_1, u_2, u_3 x_1, x_2, x_3-direction displacement in TSDT
$\bar{u}_1$, $\bar{u}_2$, $\bar{u}_3$ x_1, x_2, x_3-direction displacement in CLT
s time
Q_{x_1}, Q_{x_2} x_1, x_2-direction rotation in FSDT
κ_1, κ_2 parameters referred to as tracers
N_{ij} normal and shear force resultants
$\bar{M}_{ij}$ moment resultants
$\bar{Q}_{ij}$ transverse force resultants
F distributed load
m number of layers
$\rho^{(k)}$ mass density of the kth layer
t thickness of plates
$P_{x_1x_1}$, $P_{x_2x_2}$, $P_{x_1x_2}$ third order axial force resultants
R_{x_1}, R_{x_2} third order transverse force resultants
$\epsilon^{(0)}$, $\epsilon^{(1)}$, $\epsilon^{(3)}$ membrane strains, curvatures, and their high order strains
γ_0, γ_2 transverse shear strains and their third order terms
ψ_i^e, φ_i^e Lagrange and Hermite interpolation functions
Δ_i^e nodal values associated with $\bar{u}_3$
$K_{ij}^{\alpha\beta}$, $M_{ij}^{\alpha\beta}$ stiffness and mass coefficients
Δ interval between n loads
v moving velocity
S_k, δ_{sk} time lag and moving distance for the kth moving load
$\bar{N}_k^d$ location number of the element which the kth moving load passes through
$N_{x_1}^d$, $N_{x_2}^d$ number of division elements in the transverse and longitudinal direction
$\gamma_f(x)$ initial coordinate of the moving load in the transverse direction
L_{x_1}, L_{x_2} length of a plate in both directions
$R_{N_k}(s)$ nodal loads using the Hermite interpolation functions
(ξ_k, η_k) natural coordinates of the element
$\mathbf{\Theta}$ total magnitude of the external force
λ_0, λ_2, λ_3, λ_6, λ_7 integration constants in the Newmark integration method
$\bar{K}$ triangularized effective stiffness matrix
p uniformly distributed step load
k_{ds} dynamic magnitude factor
w_{d}, w_{s} maximum dynamic and static displacements

beam, considering the basic vibration mode and viscous damping. Veletsos and Huang (1970) analyzed a three-span continuous bridge by using various parameters such as vehicle velocity, axis spacing, the weight ratio between the vehicle and bridge, and dynamic characteristics of vehicles. Recently, various researches are conducted on vehicle-induced vibrations of bridges (Chu et al., 1986; Hwang and Nowark, 1991; Chatterjee et al., 1994; Yang and Yau, 1997). Gbandeyan and Oni (1995) analyzed a finite Rayleigh beam and a non-Mindlin rectangular plate under an arbitrary number of concentrated moving masses. Lee et al. (2002) analyzed the dynamic response of a prestressed concrete box girder bridge subjected to moving loads using folded plate elements. However, all these works are limited, in that they analyzed only structures idealized by a isotropic beam or plate member.

Many finite element analyses of anisotropic plates using first and third order shear deformation theory have been carried out but they are mostly applicable to structures under the impact or step loads (Krishna, 1977; Bhimaraddi and Stevens, 1984; Reddy and Phan, 1985; Murthy, 1981; Kant et al., 1990). In general, a first order shear deformation theory (FSDT) can describe easily and accurately the kinematic behavior of a composite plate (Reddy, 1997). However, it requires an estimation of shear correction factors; a value of $K = 5/6$ is normally used (Khdeir and Reddy, 1991). On the other hand, a third order plate theory (TSDT) is free from such requirements and thus can yield more accurate results for both static and dynamic conditions than those of the first order theories. This allows for convenient use of TSDT. Lee and Wooh (in press) extended the theory to study free vibration of composite box beams using the FEM, in which they demonstrated the criticality of the TSDT in analyzing folded composite plate structures. In this paper, the existing TSDT are adopted to study dynamic responses of composite structures subjected to various multi-moving loads, boundary conditions and layup sequences.

2. Theoretical formulation

2.1. Third order plate theory

The TSDT for analyzing laminated composite plates reviewed in this study is derived from the third-order laminate formulation of Reddy (1997). The TSDT presented in this paper is based on the same assumptions as those of the classical and first order plate theories, except that we no longer assume that the straight lines normal to the middle surface remain straight after deformation but it is assumed that they can be expressed in the form of a cubic equation. The displacement field (u_1, u_2, u_3) in cartesian coordinates (x_1, x_2, x_3) at time s for the TSDT now can be expressed as

$$\begin{aligned} u_1(x_1,x_2,x_3,s) &= \bar{u}_1(x_1,x_2,s) + x_3\phi_{x_1}(x_1,x_2,s) - \kappa_1 x_3^3(\phi_{x_1} + \kappa_0 u_{3,x_1}),\\ u_2(x_1,x_2,x_3,s) &= \bar{u}_2(x_1,x_2,s) + x_3\phi_{x_2}(x_1,x_2,s) - \kappa_1 x_3^3(\phi_{x_2} + \kappa_0 u_{3,x_2}),\\ u_3(x_1,x_2,x_3,s) &= \bar{u}_3(x_1,x_2,s), \end{aligned} \tag{1}$$

where κ_0 and κ_1 are the parameters referred to as *tracers*. The condition $\kappa_0 = 1$, $\phi_{x_1} = -u_{3,x_1}$ and $\phi_{x_2} = -u_{3,x_2}$ in Eq. (1) yields the same displacement field as that of the classical lamination theory (CLT). The displacement field becomes identical to that of FSDT for $\kappa_1 = 0$. Note that $\kappa_0 = 1$ for TSDT. In addition, $(\bar{u}_1, \bar{u}_2, \bar{u}_3)$ and (ϕ_{x_1}, ϕ_{x_2}) have the same physical meaning as in the the FSDT and denote the displacements and rotations of transverse normals on the plane $x_3 = 0$.

The equations of motion for the TSDT are derived using the principle of virtual displacements. The following Euler–Lagrange equations can be obtained using the calculus of variations (Reddy, 1997):

$$\begin{aligned} &N_{x_1x_1,x_1} + N_{x_1x_2,x_2} = \zeta_0\ddot{\bar{u}}_1 + \eta_1\ddot{\phi}_{x_1} - \kappa_1\zeta_3\ddot{\bar{u}}_{3,x_1},\\ &N_{x_1x_2,x_1} + N_{x_2x_2,x_2} = \zeta_0\ddot{\bar{u}}_2 + \eta_1\ddot{\phi}_{x_2} - \kappa_1\zeta_3\ddot{u}_{3,x_2},\\ &\bar{Q}_{x_1,x_1} + \bar{Q}_{x_2,x_2} + \kappa_1(P_{x_1x_1,x_1x_1} + 2P_{x_1x_2,x_1x_2} + P_{x_2x_2,x_2x_2}) + F\\ &\quad = \zeta_0\ddot{\bar{u}}_3 - \kappa_1^2\zeta_6(\ddot{\bar{u}}_{3,x_1x_1} + \ddot{u}_{3,x_2x_2}) + \kappa_1[\zeta_3(\ddot{\bar{u}}_{1,x_1} + \ddot{\bar{u}}_{2,x_1}) + \eta_4(\ddot{\phi}_{x_1,x_1} + \ddot{\phi}_{x_2,x_2})],\\ &\bar{M}_{x_1x_1,x_1} + \bar{M}_{x_1x_2,x_2} - \bar{Q}_{x_1} = \eta_1\ddot{\bar{u}}_1 + C_2\ddot{\phi}_{x_1} - \kappa_1\eta_4\ddot{u}_{3,x_1},\\ &\bar{M}_{x_1x_2,x_1} + \bar{M}_{x_2x_2,x_2} - \bar{Q}_{x_2} = \eta_1\ddot{\bar{u}}_2 + C_2\ddot{\phi}_{x_2} - \kappa_1\eta_4\ddot{u}_{3,x_2}, \end{aligned} \tag{2}$$

where N_{ij} are the normal $(i = j)$ and shear $(i \neq j)$ force resultants, $\bar{M}_{ij}$ are the moment resultants, $\bar{Q}_{ij}$ are the transverse force resultants, F is the distributed load, and

$$\bar{M}_{pq} = M_{pq} - \kappa_1 P_{pq}, \quad \bar{Q}_p = Q_p - c_2 R_p, \tag{3}$$

$$\zeta_i = \sum_{k=1}^{m} \int_{x_3 k}^{x_3 k+1} \rho^{(k)} (x_3)^i \, \mathrm{d}x_3 \quad (i = 0, 1, 2, \ldots, 6), \tag{4}$$

$$\eta_i = \zeta_i - \kappa_1 \zeta_i + 2, \quad C_2 = \zeta_2 - 2\kappa_1 \zeta_4 + \kappa_1^2 \zeta_6, \quad \kappa_1 = \frac{4}{3t^2}, \quad \kappa_2 = 3\kappa_1, \tag{5}$$

where m is the number of layers, $\rho^{(k)}$ is the mass density of the kth layer, t is the wall thickness, and $(P_{x_1 x_1}, P_{x_2 x_2}, P_{x_1 x_2})$ and (R_{x_1}, R_{x_2}) denote the higher-order resultants. The resultants are related to the strains by the relationship:

$$\begin{Bmatrix} \{N\} \\ \{M\} \\ \{P\} \end{Bmatrix} = \begin{pmatrix} [A] & [B] & [E] \\ [B] & [D] & [F] \\ [E] & [F] & [H] \end{pmatrix} \begin{Bmatrix} \{\epsilon^{(0)}\} \\ \{\epsilon^{(1)}\} \\ \{\epsilon^{(3)}\} \end{Bmatrix}, \tag{6}$$

$$\begin{Bmatrix} \{Q\} \\ \{R\} \end{Bmatrix} = \begin{pmatrix} [A] & [D] \\ [D] & [F] \end{pmatrix} \begin{Bmatrix} \{\gamma^{(0)}\} \\ \{\gamma^{(2)}\} \end{Bmatrix}, \tag{7}$$

where $\epsilon^{(0)}$ are the membrane strains, $\epsilon^{(1)}$ are the curvatures, $\epsilon^{(3)}$ are the high order strains, and $\gamma^{(0)}$ and $\gamma^{(2)}$ are the transverse shear strains and their high order terms, respectively. The stiffnesses in Eqs. (6) and (7) are given in terms of the layer stiffnesses $\bar{Q}_{ij}^{(k)}$ of the kth layer and the positions of the top and bottom faces of the kth layer $x_3 k + 1$ and $x_3 k$ as

$$(A_{ij}, B_{ij}, D_{ij}, E_{ij}, F_{ij}, H_{ij}) = \sum_{k=1}^{n} \int_{x_3 k}^{x_3 k+1} \bar{Q}_{ij}^{(k)} \left(1, x_3, x_3^2, x_3^3, x_3^4, x_3^6\right) \mathrm{d}x_3, \quad i, j = 1, 2, 6, \tag{8}$$

$$(A_{ij}, D_{ij}, F_{ij}) = \sum_{k=1}^{n} \int_{x_3 k}^{x_3 k+1} \bar{Q}_{ij}^{(k)} \left(1, x_3^2, x_3^6\right) \mathrm{d}x_3, \quad i, j = 4, 5. \tag{9}$$

Note that the stiffnesses E_{ij}, F_{ij} and H_{ij} consist of the terms whose orders are higher than cubic of the plate thickness.

2.2. Displacement finite element method

2.2.1. Finite element model

The model described by Eq. (2) is named the *displacement finite element method* by Reddy and Phan (1985), which requires the use of Lagrange interpolation of $(\bar{u}_1, \bar{u}_2, \phi_{x_1}, \phi_{x_2})$ and Hermite interpolation of $\bar{u}_3$. A nonconforming element for plates will thus have seven degrees of freedom per node, i.e., $\bar{u}_1$, $\bar{u}_2$, $\bar{u}_3$, $\bar{u}_{3,x_1}$, $\bar{u}_{3,x_2}$, ϕ_{x_1}, and ϕ_{x_2}. The generalized displacements can be approximated over an element Ω^e by the expressions

$$
\begin{aligned}
\bar{u}_1(x_1,x_2,s) &= \sum_{i=1}^{m} \bar{u}_{1i}^e(s)\psi_i^e(x_1,x_2),\\
\bar{u}_2(x_1,x_2,s) &= \sum_{i=1}^{m} \bar{u}_{2i}^e(s)\psi_i^e(x_1,x_2),\\
\bar{u}_3(x_1,x_2,s) &= \sum_{i=1}^{m} \bar{\Delta}_i^e(s)\varphi_i^e(x_1,x_2),\\
\phi_{x_1}(x_1,x_2,s) &= \sum_{i=1}^{m} X_i^e(s)\psi_i^e(x_1,x_2),\\
\phi_{x_2}(x_1,x_2,s) &= \sum_{i=1}^{m} Y_i^e(s)\psi_i^e(x_1,x_2),
\end{aligned}
\tag{10}
$$

where ψ_i^e denote the Lagrange interpolation functions and φ_i^e are the Hermite interpolation functions. For the nonconforming elements, the three nodal values associated with $\bar{u}_3$ are written as $\bar{\Delta}_1 = \bar{u}_3$, $\bar{\Delta}_2 = \bar{u}_{3,x_1}$, $\bar{\Delta}_3 = \bar{u}_{3,x_2}$.

These equations can be rewritten in compact form as

$$
\sum_{\beta=1}^{5}\sum_{j=1}^{n_\beta}\left(K_{ij}^{\alpha\beta}\Delta_j^\beta + M_{ij}^{\alpha\beta}\ddot{\Delta}_j^\beta\right) - F_i^\alpha = 0, \quad i = 1,2,\ldots,n_\alpha, \tag{11}
$$

where $\alpha = 1, 2, 3, 4, 5$, $n_1 = n_2 = n_4 = n_5 = 4$, and $n_3 = 12$ for nonconforming elements, Δ_j^β denote the nodal values, $K_{ij}^{\alpha\beta}$ are the stiffness coefficients, $M_{ij}^{\alpha\beta}$ are the mass coefficients, and F_i^α are the external forces, respectively.

2.2.2. Multi-moving loads

Based on the assumption of small deformations, the dynamic response of a laminated composite plate caused by a series of movings can be obtained as the superposition of the response induced by each of the moving loads. In this study, Newmark's explicit integration technique is adopted for the transient analysis (Bathe, 1996).

Consider n loads of interval Δ at moving velocity v as shown in Fig. 1. The total traveling time (s) of the loads can be obtained as

$$
s_d\ (\mathrm{s}) = 3.6\left(\frac{L_{x_2} + \Delta_1 + \Delta_2 + \cdots + \Delta_{n-1}}{v}\right). \tag{12}
$$

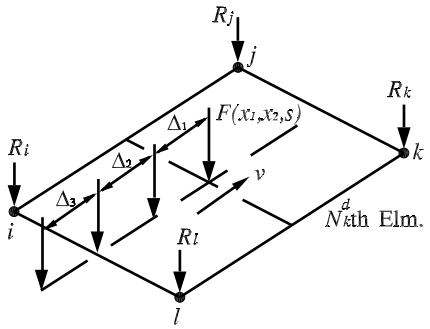

Fig. 1. Multi-moving loads at arbitrary N_kth plate element.

Assuming that the first moving load enters the plate at $s = 0$, the time lag (s) for the kth moving load is $s_k = 3.6(k-1)\Delta/v$. Thus, the moving distance (m) for kth moving load at time $s + \Delta s$ is $\delta_{sk} = vs_k$. The location number $\bar{N}_k^d$ of the element which the kth moving load passes through at time $s + \Delta s$ can be expressed as

$$^{s+\Delta s}\bar{N}_k^d = I_l(N_{x_1}^d - 1) + I_s + 1, \tag{13}$$

where

$$I_l = \mathbf{INT}\left(\frac{^{s+\Delta s}\delta_{sk}N_{x_2}^d}{L_{x_2}}\right) \quad \text{and} \quad I_s = \mathbf{INT}\left(\frac{\gamma_f(x)N_{x_1}^d}{L_{x_1}}\right). \tag{14}$$

Here, $N_{x_1}^d$ and $N_{x_2}^d$ are the number of division elements in the transverse and longitudinal direction, $\gamma_f(x)$ is the initial coordinate of the moving load in the transverse direction, L_{x_1} and L_{x_2} are the length of a plate in both directions, respectively.

The moving load vectors $\{F_k(s)\}$ at an arbitrary location on the N_k^dth element of the plate should be inevitably distributed to the nodal loads $\{R_{N_k}(s)\}$ using the Hermite interpolation function $[\Phi]$. The natural coordinates (ξ_k, η_k) of the element for the k th moving load at time $s + \Delta s$ can be derived as

$$^{s+\Delta s}\xi_k = 2\left(\frac{\gamma_f(x_1)N_{x_1}^d}{L_{x_1}} - I_s\right) - 1 \quad \text{and} \quad ^{s+\Delta s}\eta_k = 2\left[\frac{(\gamma_f(x_2) + ^{s+\Delta s}\delta_{sk})N_{x_2}^d}{L_{x_2}} - I_l\right] - 1. \tag{15}$$

In four-node element for seven degrees of freedom per a node, the distributed kth moving loads toward near four nodes can be expressed as

$$^{s+\Delta s}\mathbf{R}_{N_k} = \begin{Bmatrix} S_j \\ S_{j+1} \\ S_{j+2} \end{Bmatrix} = [F_k][I]\begin{Bmatrix} \Phi_j(\xi_k, \eta_k) \\ \Phi'_{j+1}(\xi_k, \eta_k) \\ \Phi''_{j+2}(\xi_k, \eta_k) \end{Bmatrix}, \tag{16}$$

where $j = 7(i-1) + 2$ for $i = 1, \ldots, 4$.

The total magnitude $\mathbf{\Theta}$ of the external force applied on the plate at $s + \Delta s$ can be obtained by summing up the distributed N loads as given by

$$^{s+\Delta s}\mathbf{\Theta} = ^{s+\Delta s}\mathbf{\Theta}_{N_1} + ^{s+\Delta s}\mathbf{\Theta}_{N_2} + \cdots + ^{s+\Delta s}\mathbf{\Theta}_{N_n}. \tag{17}$$

In Newmark integration scheme the effective loads at time $s + \Delta s$ can be calculated as

$$^{s+\Delta s}\bar{\mathbf{\Theta}} = ^{s+\Delta s}\mathbf{\Theta} + \mathbf{M}(\lambda_0{}^s\mathbf{U} + \lambda_2{}^s\dot{\mathbf{U}} + \lambda_3{}^s\ddot{\mathbf{U}}). \tag{18}$$

The dynamic displacements $\mathbf{U}$, accelerometers $\ddot{\mathbf{U}}$, and velocities $\dot{\mathbf{U}}$ at time $s + \Delta s$ can be solved as

$$^{s+\Delta s}\mathbf{U} = [\bar{\mathbf{K}}^{-1}]^{s+\Delta s}\bar{\mathbf{\Theta}}, \tag{19}$$

$$^{s+\Delta s}\ddot{\mathbf{U}} = \lambda_0(^{s+\Delta s}\mathbf{U} - {}^s\mathbf{U}) - \lambda_2^s\dot{\mathbf{U}} - \lambda_3\ddot{\mathbf{U}} \quad \text{and} \quad ^{s+\Delta s}\dot{\mathbf{U}} = {}^s\dot{\mathbf{U}} - \lambda_6{}^s\ddot{\mathbf{U}} - \lambda_7^{s+\Delta s}\ddot{\mathbf{U}}, \tag{20}$$

where the triangularized effective stiffness matrix is $\bar{\mathbf{K}} = \mathbf{K} + \lambda_0\mathbf{M}$, λ_0, λ_2, λ_3, λ_6, and λ_7 are integration constants in the Newmark integration method, respectively.

3. Numerical results and discussion

The finite element formulation described in the earlier section was used to compare the present results using TDST and FDST with the published result and also to generate numerical results to study the effects

of various moving velocities, fiber angles, and boundary conditions on the dynamic behaviors of laminated composite plates. In this study, two types of plates and stacking sequences are used. The composite plates are simply supported single and two continuous spans such as slab bridges. The stacking sequences in this study are classified into symmetric and antisymmetric angle plies. Based on TSDT, the classified parametric cases are applied to analyze dynamic responses for single, three and five moving loads, respectively. The computer program developed in this study is coded by using Fortran 95 (Lahey). It is composed of a static analysis module, free vibration analysis module and dynamic analysis module for a moving load. It has the advantage that the user can manage the in-output file without primary difficulty by using the Hoit method. A flow chart of the computational procedure is shown in Fig. 2. Dimensions and boundary conditions of a single or two-span composite plate are shown in Fig. 3. In the figure, note that $u_1 = u_2 = u_3 = 0$ (S.S.E.) at $a/2$ for the two-span continuous plate.

3.1. Comparison of results obtained by FDST and TDST

To check the accuracy of the code developed and the difference of results between FDST and TDST, the central deflection of a [0/90/0] composite plate (Model I) subjected to a uniformly distributed step load for all clamped boundary condition has been obtained using this code. The material properties and input parameters used in this study are listed in Table 1. In the case of FSDT, the results conform satisfactorily to those of Kant et al. (1990) as shown in Fig. 4. On the other hand, the results analyzed by using TSDT are different from those analyzed by using FDST. The discrepancies between the results analyzed by TSDT and FSDT shown in Fig. 4 are caused by the effects of third order terms such as E_{ij}, F_{ij}, and H_{ij} in TSDT. Because of these terms, the deformation of a transverse normal according TDST is nonlinear. On the other hand, in the case of FSDT, it normally uses assumed shear correction factors (generally 5/6) instead of the third order terms. For these reasons, the difference can occur in the results between FSDT and TSDT in the figure. As pointed out in Introduction, FSDT can describe easily and accurately the kinematic behaviors of a composite plate. However, the dynamic responses of composite plates in different plate theories depend on various material properties and geometries of plates, especially for the side-to-thickness ratio or boundary conditions (Lee and Wooh, in press).

3.2. Single composite plate

Fig. 5 shows the dynamic displacements of symmetric cross-ply single composite plate (Model I) under the single moving load with two different velocities and plate theories. In Fig. 5, we can observe noticeably different results depending on fiber angles, moving velocities and plate theories. For two different plate theories, the maximum difference of dynamic displacements between TSDT and FSDT is about 10% for the fiber angle [45/−45/45/−45], which is relatively bigger than that of [0/90/90/0]. From Fig. 5, it can be also observed that the 120 km/h moving velocities and [45/−45/−45/45] ply angle lamination produce the lowest frequencies along longitudinal length of the plate. On the other hand, the dynamic displacement induced for [45/−45/−45/45] ply angle is higher than that of [0/90/90/0]. Finally, Fig. 5 shows a comparative study of results obtained applying TSDT and FDST for different moving velocities and ply angles. The figure also reveals that there is perceptible difference in the results for different theories, and the third term of transverse shear deformation may be employed for better computational accuracy.

Fig. 6 shows dynamic response of antisymmetric cross-ply composite single plates subjected to three moving loads for different velocities (a), (b) and (c). As the moving velocity increases, the shape of the dynamic displacements becomes smoother. This is predictable because it is expected that a faster moving velocity would increase the moving distance per unit time. For the ply angle of [0/90/0/90], the induced

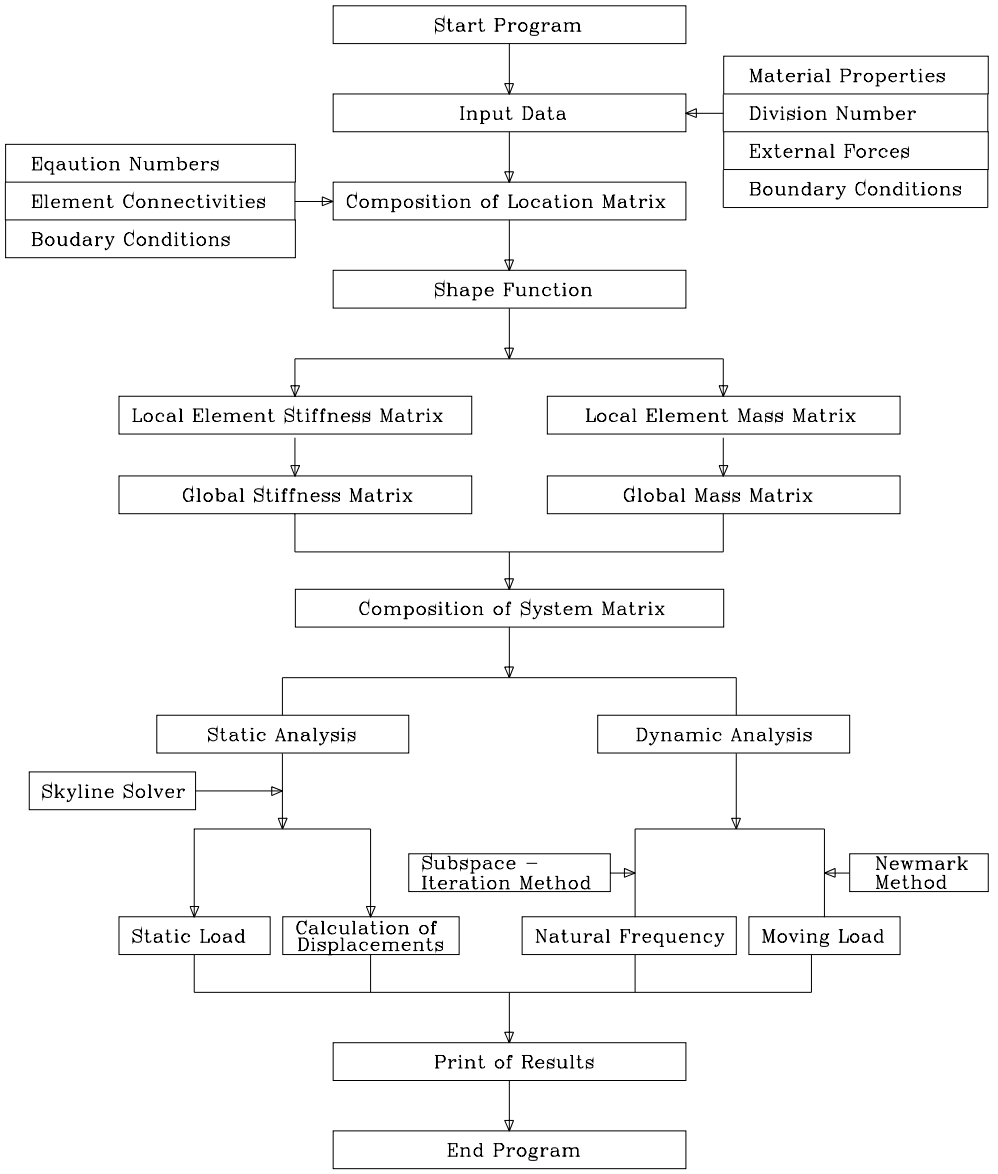

Fig. 2. A flow chart for determining static and dynamic responses of composite plate under the moving loads.

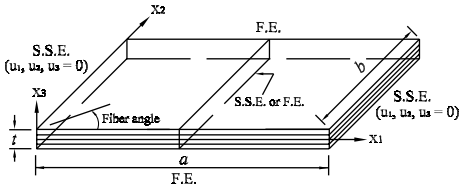

Fig. 3. Dimensions and boundary conditions of a laminated composite plate analyzed by the TSDT. S.S.E. and F.E. denote simply supported and free edges, respectively.

Table 1
Materials properties and input parameters used in this study

Model	E_1	E_2	G_{12}	G_{23}	G_{13}	v_{12}	ρ	a	b	t	F	Δs
I	52.50	$E_1/25$	10.5	10.5	10.5	0.25	800	0.25	0.25	0.05	10.0	5.0
II	60.70	24.80	12.0	12.0	12.0	0.23	1300	10.0	0.5	5.0	1.0	5000.0

For material properties, the units of E_1, E_2, G_{12}, G_{23}, G_{13} are GPa and that of ρ is kg/m^3, respectively. For input parameters, the units of a, b, t are m, that of F is N/cm^2 (Model I) or tonf (Model II), and that of Δs is μ s, respectively. Note that $a = 20.0$ for two-span continuous plates of Model II.

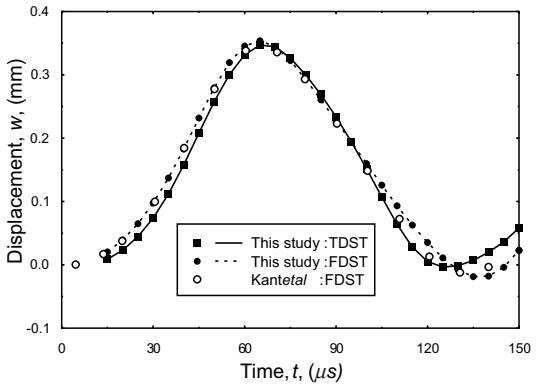

Fig. 4. Comparison of dynamic responses of a [0/90/0] composite plate (Model I) subjected to a uniformly distributed step load for all clamped boundary condition. The displacement at the center of the plate is computed for every 5 μs.

displacements are smaller than the others regardless of moving velocities, because it has the highest bending stiffness in the longitudinal direction. For two-span continuous composite plates, the trends of the displacement with different ply angles are similar to those of single plates as shown in Fig. 7. This observation provides us with a clue that it would be better to use the [0/90/0/90] ply orientation for antisymmetric plies in designing the structures subjected to moving loads such as composite bridge decks.

Dynamic analysis of single composite plates under five moving loads with symmetric cross-ply lamination are performed to determine the *dynamic magnitude factor* (DMF, κ_{ds}) as shown in Table 2 (Lee et al., 2002). We can observe that the [0/90/90/0] laminate exhibits the lowest maximum displacements and DMF regardless of moving velocities. In particular, it may be noticed that the maximum displacements of the [30/−60/−60/30] laminate are approximately three times as much as those of the [90/0/0/90] laminate even for the same material properties. On the other hand, in the case of antisymmetric layup sequences shown in Table 3, the [0/90/0/90] laminate (=[90/0/0/90]) shows the lowest maximum displacements. The significant difference in the results between symmetric and antisymmetric laminates depends on the magnitude of B_{ij} and E_{ij} in Eq. (7). In the case of symmetric cross-ply laminates, the coupling stiffnesses B_{ij} and E_{ij} become zero. On the other hand, it should be noted that they become nonzero for antisymmetric laminates. The coupling nonzero terms caused by antisymmetric laminates can make deleterious contributions to the overall dynamic behaviors of the plate. On the other hand, the DMF of [45/−45/45/−45] laminate is smaller than that of [45/−45/−45/45] laminate. For other cases, the lowest magnitudes of the DMFs are different with increasing moving velocities for the different layup sequences. Furthermore, we can observe that the DMFs for most different ply angles are less than 1.2 regardless of moving velocities. This result may allow us to consider that the plates made of composite materials have excellent dynamic resistance for most ply angles. Among them, the usage of [90/0/0/90] laminate is recommended.

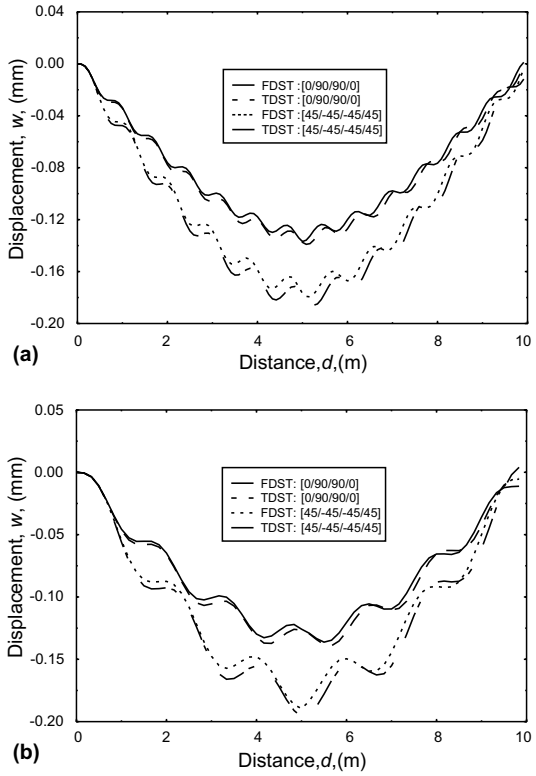

Fig. 5. Dynamic responses of [0/90/90/0] and [45/−45/−45/45] composite single plate (Model II) subjected to single load for different velocities (a) and (b). The displacement at the center of the plate is computed for every 0.005 s. The velocity of single load is (a) 60 km/h, (b) 120 km/h.

3.3. Two-span continuous composite plate

Fig. 8 shows maximum dynamic displacements of two-span continuous composite plates subjected to multi-moving loads for different velocities and symmetric layup sequences. It can be observed that the maximum displacements of [90/0/0/90] laminate are noticeably smaller than others regardless of the moving velocities. On the other hand, the DMFs for each laminate make little differences regardless of moving velocities as shown in Fig. 9. Finally, Figs. 8 and 9 reveal that [90/0/0/90] laminate has superior stiffness for moving loads, but the differences between [90/0/0/90] and others in the rigidity for the dynamic effects are negligible. In the case of antisymmetric case, it can be observed from Fig. 10 that the maximum displacements of [0/90/0/90] laminate are relatively smaller than others regardless of moving velocities. However, it may be noted from Figs. 8 and 10 that they are larger than those of [90/0/0/90]. This is similar to that of symmetric layup sequence shown in Tables 2 and 3. The DMFs (Fig. 11) for each laminate are also similar to that shown in Fig. 9. As we mentioned earlier, the dynamic effects attributed to the zero terms B_{ij} and E_{ij} of the [90/0/0/90] laminate have better influence on the dynamic behaviors. This observation provides us with a clue that it could be better to use [90/0/0/90] ply orientations in designing both single and two-span continuous composite plates subjected to moving loads. However, we should recall that dynamic effects by the coupling terms could be dependent on other factors such as the shape and material properties of a plate.

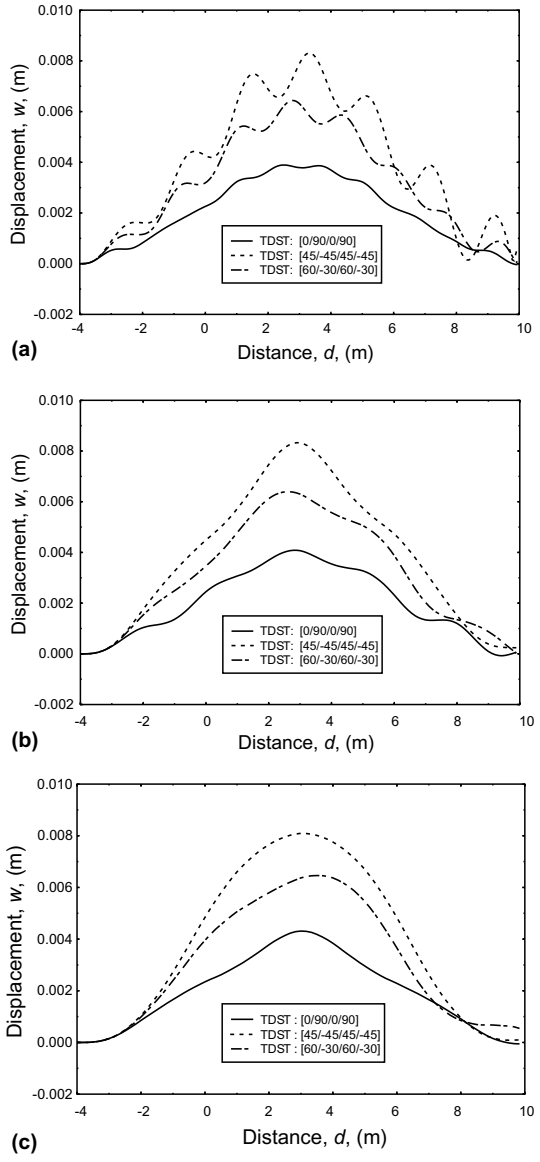

Fig. 6. Dynamic response of [0/90/0/90], [45/−45/45/−45] and [60/−30/60/−30] composite single plates (Model II) subjected to three moving loads for different velocities (a), (b) and (c). The displacement at the center of the plate is computed for every 0.005 s. The velocities of three moving loads are (a) 40 km/h, (b) 80 km/h, (c) 120 km/h.

4. Summary and conclusion

An intuitive prediction of the dynamic behavior of composite structures subjected to multi-moving loads is difficult because of their complexity due to the combined effect of anisotropy. In this study, the dynamic characteristics are analyzed by considering various parameters. The advanced transient vibration analysis based on the third order plate theory shows the significance of stacking sequences and moving velocities of the load for composite plates with various boundary conditions.

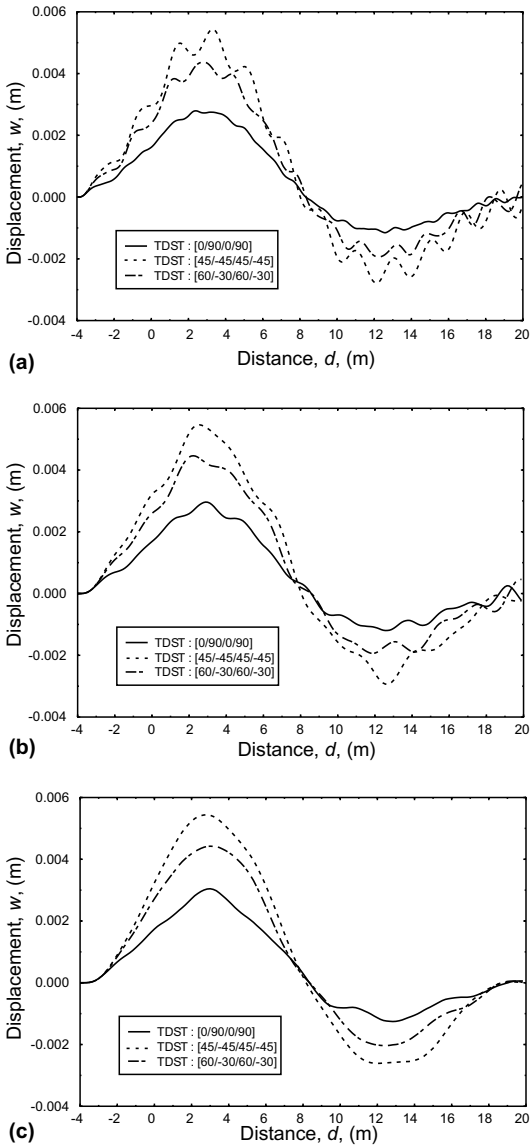

Fig. 7. Dynamic response of [0/90/0/90], [45/−45/45/−45] and [60/−30/60/−30] composite plates (Model II) subjected to multi-moving loads for different velocities (a), (b) and (c). The displacement at the center of the plate is computed for every 0.005 s. The velocities of three moving loads are (a) 40 km/h, (b) 80 km/h, (c) 120 km/h.

The parametric case studies revealed the importance of layup sequences for efficient and economic design. The following key observations were made in designing single and two-span continuous composite structures under the moving loads.

1. The dynamic responses of composite plates analyzed by TSDT and FSDT were significantly different from each other for different moving velocities and fiber orientations. It was especially true for

Table 2
Dynamic effects of composite plate (Model II) with single span for different velocities and symmetric layup sequences

Layup sequence	Dynamic effect	Moving velocity (km/h)						
		20	40	60	80	100	120	140
[0/90/90/0]	w_d	8.271	8.781	8.375	8.403	8.464	8.747	8.396
	w_s	8.206	8.206	8.206	8.206	8.206	8.206	8.206
	κ_{ds}	1.007	1.070	1.021	1.024	1.031	1.066	1.023
[30/−60/−60/30]	w_d	10.890	11.628	10.296	10.040	10.789	10.509	10.357
	w_s	10.125	10.125	10.125	10.125	10.125	10.125	10.125
	κ_{ds}	1.076	1.148	1.069	0.991	1.066	1.038	1.023
[45/−45/−45/45]	w_d	9.854	10.635	9.371	9.262	9.838	9.735	9.267
	w_s	8.207	8.207	8.207	8.207	8.207	8.207	8.207
	κ_{ds}	1.201	1.295	1.142	1.128	1.199	1.186	1.129
[90/0/0/90]	w_d	3.318	3.337	3.347	3.477	3.309	3.389	3.272
	w_s	3.312	3.312	3.312	3.312	3.312	3.312	3.312
	κ_{ds}	1.002	1.007	1.010	1.049	0.999	1.023	0.987

Table 3
Dynamic effects of composite plate (Model II) with single span for different velocities and antisymmetric layup sequences

Layup sequence	Dynamic effect	Moving velocity (km/h)						
		20	40	60	80	100	120	140
[0/90/0/90]	w_d	4.939	4.830	5.387	4.808	4.856	4.692	4.962
	w_s	4.731	4.731	4.731	4.731	4.731	4.731	4.731
	κ_{ds}	1.044	1.021	1.139	1.016	1.026	0.992	1.049
[30/−60/30/−60]	w_d	7.304	7.430	7.375	7.446	7.380	7.739	7.552
	w_s	7.260	7.260	7.260	7.260	7.260	7.260	7.260
	κ_{ds}	1.006	1.023	1.016	1.025	1.016	1.065	1.040
[45/−45/45/−45]	w_d	9.737	10.541	9.279	9.214	9.755	9.683	9.158
	w_s	9.213	9.213	9.213	9.213	9.213	9.213	9.213
	κ_{ds}	1.057	1.144	1.007	1.000	1.059	1.051	0.994
[75/−15/75/−75]	w_d	5.392	5.398	5.843	5.381	5.478	5.492	5.701
	w_s	5.365	5.365	5.365	5.365	5.365	5.365	5.365
	κ_{ds}	1.005	1.006	1.089	1.003	1.021	1.024	1.063

[45/−45/45/−45]. In this case, the moving velocities made greater contributions to the dynamic responses of composite plates for higher speed.

2. We found that the maximum displacement of [90/0/0/90] laminates are noticeably smaller than others regardless of the moving velocities. On the other hand, the usage of [45/−45/−45/45] or [45/−45/45/−45] ply angle should be avoided for almost any conditions because of its undesirable dynamic response. For the single and two-span continuous plates, the trends of the displacement with different ply angles are similar to each other.
3. On the other hand, differences in dynamic resistance (DMF) for different ply angles are negligible both in single and two-span continuous plates. The DMFs are less than 1.2 for most ply angles and moving velocities. This result reveals that the dynamic resistance for plates made of composite materials is excellent and stable. In particular, the usage of [90/0/0/90] laminate is recommended.
4. Because of the effect of the coupling stiffnesses B_{ij} and E_{ij}, the maximum of symmetric laminates to dynamic loading is superior to that of the antisymmetric laminates. However, the DMF for antisymmetric

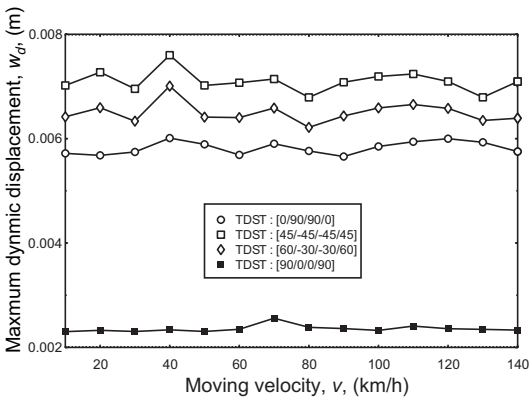

Fig. 8. Maximum dynamic displacements of two-span continuous composite plates (Model II) subjected to multi-moving loads for different velocities and symmetric layup sequences. The displacement at the center of the plate is computed for every 0.005 s.

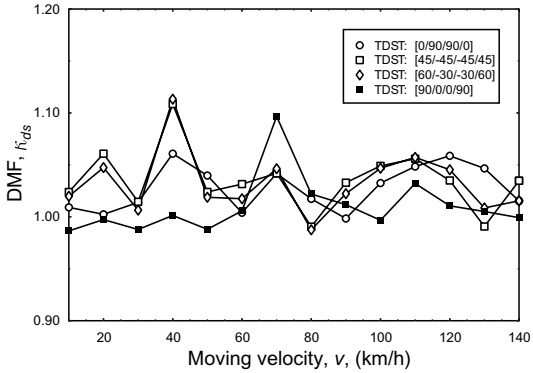

Fig. 9. Maximum magnitude factors of two-span continuous composite plates (Model II) subjected to multi-moving loads for different velocities and symmetric layup sequences. The displacement at the center of the plate is computed for every 0.005 s.

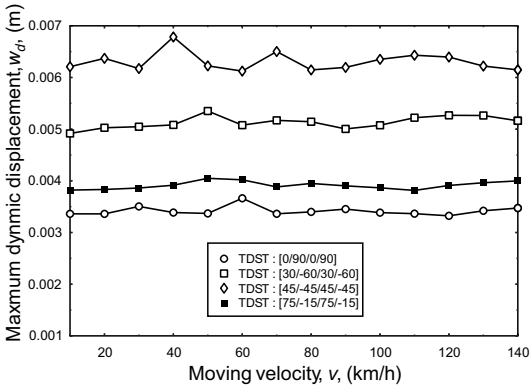

Fig. 10. Maximum dynamic displacements of two-span continuous composite plates (Model II) subjected to multi-moving loads for different velocities and antisymmetric layup sequences. The displacement at the center of the plate is computed for every 0.005 s.

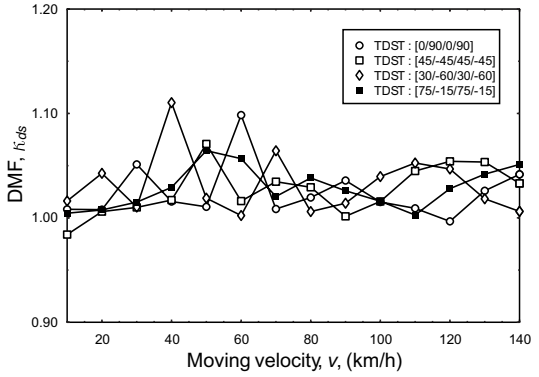

Fig. 11. Maximum magnitude factors of two-span continuous composite plates (Model II) subjected to multi-moving loads for different velocities and antisymmetric layup sequences. The displacement at the center of the plate is computed for every 0.005 s.

layup sequences are similar to that of the symmetric cases both in single and two-span continuous cases. In this case, B_{ij} and E_{ij} of antisymmetric laminates make positive contributions on the stable dynamic resistance.

With the advancement of technology in fiber-reinforced composite materials, the applicability of composites to bridge decks has been increased. The results of this study may serve as a benchmark for future guidelines in designing composite structures subjected to various moving loads. But our parametric study is only an example, and more studies should be carried out for individual design cases.

References

Bathe, K.J., 1996. The Finite Element Procedures in Engineering Analysis. Prentice Hall, NJ, USA.

Biggs, J.M., 1959. Vibrations of simple span highway bridges. Trans., ASCE, 124.

Chatterjee, P.K., Datta, T.K., Surana, C.S., 1994. Vibration of suspension bridges under vehicular movement. J. Struct. Eng., ASCE 120, 681–703.

Chu, K.H., Garg, V.K., Wang, T.L., 1986. Impact in railway prestressed concrete bridges. J. Struct. Eng., ASCE 112, 1036–1051.

Gbandeyan, J.A., Oni, S.T., 1995. Dynamic behaviour of beams and rectangular plates under moving loads. J. Sound Vib. 182 (5), 677–695.

Hwang, E.S., Nowark, A.S., 1991. Simulation of dynamic load for bridges. J. Struct. Eng., ASCE 117, 1413–1434.

Jeffcott, H.H., 1929. On the vibrations of beam under the action of moving loads. Philos. Mag., Series 7 8, 66–97.

Kant, T., Varaiya, J.H., Arora, C.P., 1990. Finite element transient analysis of composite and sandwich plates based on a refined theory and implicit time integration schemes. Comp. Struct. 36 (3), 401–420.

Khdeir, A.A., Reddy, J.N., 1991. Analytical solutions of refined plate theories of cross-ply composite laminates. J. Pressure Vessel Technol. 113, 570–578.

Krishna, M.A.V., 1977. Higher order theory for vibration of thick plates. Am. Inst. Aeronaut. Astronaut. J. 15, 1823–1824.

Lee, R.C., Lee, S.Y., Yhim, S.S., 2002. A study on the dynamic responses of PSC box girder bridge under the moving load. In: Proc. First International Conference on Bridge Maintenance Safety and Management, Spain.

Lee, S.Y., Wooh, S.C. Finite element vibration analysis of composite box structures using the high order plate theory. J. Sound Vib., in press.

Looney, C.T.G., 1958. Hi-speed computer applied to bridge impact. In: Proc. ASCE. 84, ST5.

Lowan, A.N., 1935. On transverse oscillations of beams under the action of moving variable loads. Philos. Mag., Series 7 19, 708.

Murthy, M.V.V., 1981. An improved transverse shear deformation theory for laminated anisotropic plates. NASA Technical Paper 1903, pp. 1–37.

Reddy, J.N., 1997. Mechanics of Laminated Composite Plates: Theory and Analysis. CRC Press, NY, USA.

Reddy, J.N., Phan, N.D., 1985. Stability and vibration of isotropic, orthotropic, and laminated plates according to a higher-order shear deformation theory. J. Sound Vib. 98, 157–170.

Stokes, G.G., 1849. Discussion of a differential equation related to the breaking of railway bridges. Trans. Cambridge Philos. Soc. 8, 707–735.

Timoshenko, S.P., 1922. On the forced vibration of bridges. Philos. Mag., Series 6 43, 1018–1019.

Veletsos, A.S., Huang, T., 1970. Analysis of dynamic response of highway bridges. J. Eng. Mech., ASCE 96, 593–620.

Willis, R., 1849. Appendix to the report of the commissioners appointed to inquire into the application of iron to railway structures. Stationary Office, London, UK.

Yang, Y.B., Yau, J.D., 1997. Vehicle-bridge interaction element for dynamic analysis. J. Struct. Eng., ASCE 123, 1512–1518.